Magnon Polariton and Pseudo-Magnon-Polariton

C.-M. Hu*, B. M. Yao*†, S. Kaur*, Y. S. Gui*, and W. Lu†
*Department of Physics and Astronomy, University of Manitoba, Winnipeg, Manitoba R3T 2N2, Canada
†National Laboratory for Infrared Physics, Chinese Academy of Sciences, Shanghai 200083, People's Republic of China.

***Abstract*—Experimental realization of magnon-photon coupling in microwave cavity is leading to a new field of cavity spintronics, which paves new ways for microwaves and materials applications utilizing magnon polariton and pseudo-magnon-polariton.**

I. Introduction and Background

VIA electrodynamic coupling, the high-frequency magnetic field of microwave is coupled with magnetization dynamics in magnetic materials, which forms the magnon polariton. Of particular interest is the the cavity magnon polariton that can be created by inserting a low damping magnetic insulator into a high-quality microwave cavity. Interesting dynamic features such as the forming of a polariton gap, Rabi-like oscillation, magnetically induced transparency, and the Purcell effect have recently been demonstrated. A new field of cavity spintronics is emerging which explores the physics and applications of magnon-photon coupling [1]–[5].

II. Results

In this section, we will briefly review our recent work in this frontier of condensed matter and wave physics by addressing the following topics: (1) cavity magnon-polariton,(2) voltage-controlled pseudo-magnon-polariton for creating tunable electromagnetically induced transparency (EIT) and (3) characterization of magnetic nanoparticles (MNP) by using magnon-photon coupling effect. These results will be presented and demonstrate how the research of the fundamental physics can pave new ways for practical applications.

A. Magnon Polariton

Magnon polaritons are quasiparticles resulting from coupling of electromagnetic waves with collective excitation of the electrons' spin in ferromagnetic materials and structures. To observe the magnon polariton, a ferrite YIG sample with a thickness of l_s=0.5 mm and a cross section of about 5.5×3.5 mm^2, is loaded in the center of the waveguide assembly (with a total length of $2l = 85$ mm) as shown in Fig. 1(a). The microwave cavity used in this experiment is a Fabry-Perot-liked resonator based on the Ku-band (12 GHz- 18 GHz) assembled waveguide apparatus [6], where circular waveguides are connected through circular-rectangular transitions to coaxial-rectangular adapters and two transitions are rotated by an angle θ. The fundamental mode for the rectangular waveguide is TE10, while that for the circular waveguide is TE11, supporting two degenerate orthogonal waves. Based on the polarization direction in the each component of the waveguide assembly a Fabry-Perot-liked resonator is built, and the analytic solution of wave propagation has been deduced based on Maxwell's equation as detailed in the discussion in Ref. [6]. The microwave propagation in such an apparatus can be characterized by the S-parameter and measured by a vector network analyzer (VNA).

A static magnetic field was applied in the x-y plane, perpendicular to the direction of wave propagation. The dynamic response of the magnetization precession $\mathbf{m}$ driven by the microwave magnetic field $\mathbf{h}$ is phenomenologically governed by the Landau-Lifshitz-Gilbert (LLG) equation expressed as

$$\frac{d\mathbf{M}}{dt} = -\gamma(\mathbf{M} \times \mathbf{H}_i) + \frac{\alpha}{M_0}\left(\mathbf{M} \times \frac{d\mathbf{M}}{dt}\right). \qquad (1)$$

Here $\gamma = \mu_0 e/m_e$ is the effective gyromagnetic ratio of an electron (charge e and mass m_e), α is the Gilbert damping parameter, M_0 is the saturation magnetization. Inside the ferrite sample, the magnetization $\mathbf{M} = \mathbf{M_0} + \mathbf{m}$ and magnetic field $\mathbf{H}_i = \mathbf{H}_{ext} + \mathbf{h}$ consist of static components $\mathbf{M_0}$ and $\mathbf{H}_{ext}$ as well as the dynamic components $\mathbf{m}$ and $\mathbf{h}$ including time dependent term $e^{-i\omega t}$. Meanwhile, the wave propagation in the insulating ferrite should also follow the Maxwell's equation

$$\nabla^2\mathbf{h} - \varepsilon_s\varepsilon_0\mu_0\omega^2\mathbf{h} = \nabla(\nabla \cdot \mathbf{h}) + \varepsilon_s\varepsilon_0\mu_0\omega^2\mathbf{m}, \qquad (2)$$

where ε_s, ε_0 and μ_0 are the relative complex permittivity, vacuum permittivity and vacuum permeability, respectively.

By solving the coupling Eqs. (1) and (2), the final transmission coefficient near the ferromagnetic resonance (FMR), at which the microwave electric field tends to be zero at the center of the waveguide assembly cavity, then reduces to

$$S_{21} \propto 1 + \frac{\Delta\omega_1}{i(\omega - \omega_1) - \Delta\omega_1 + \frac{\kappa^2}{i(\omega-\omega_2)-\Delta\omega_2}} \qquad (3)$$

where ω_1 (ω_2) is the resonance frequency for the cavity mode(FMR mode),$\Delta\omega_1 = (c/6l)\sqrt{1-(\omega_c/\omega_1)^2}$ ($\Delta\omega_2 = \alpha(\omega_H + \omega_M/2)$) is its damping coefficient, and $\kappa^2 = (l_s/4l)[1-(\omega_c/\omega_1)^2](\omega_H + \omega_M)\omega_M$ is the coupling strength between the cavity mode and FMR mode. ω_c is the cut-off frequency of the circular waveguide and $\omega_H = \gamma H_{ext}$ and $\omega_M = \gamma M_0$. For our YIG sample γ=169.0 μ_0 GHz/T, μ_0M$_0$=0.154 T and α= 0.125% are experimentally determined.

Figure 1(b) shows how the ferromagnetic resonance of YIG couples with the microwave cavity mode. Here the dotted line is the expected FMR dispersion of YIG calculated from Kittel's formula $\omega_2 = \gamma\sqrt{H_{ext}(H_{ext} + M_0)}$ and the dashed line is the cavity mode at $\omega_1/2\pi$=12.16 GHz. When the resonance frequency difference between the FMR mode and

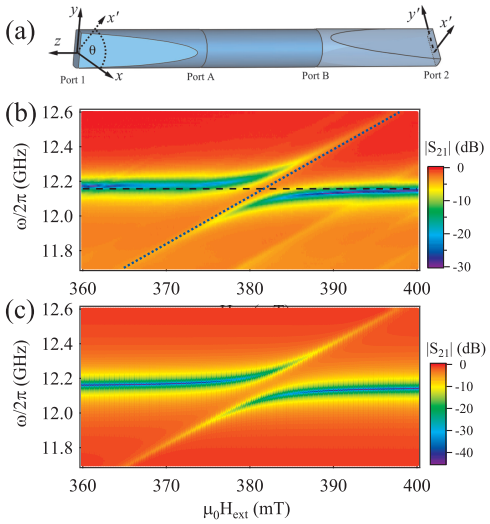

Fig. 1. (a)Schematic of the waveguide assembly cavity. Two circular-rectangular transitions are twisted by an angle θ with respect to each other and are connected to a vector network analyzer. (b) The measured and (c) the calculated dispersion of a magnon polariton formed by inserting a ferromagnetic insulator sample made of yttrium iron garnet(YIG) into a high quality microwave cavity. At the external magnetic field of about 380 mT, the ferromagnetic resonance of YIG couples with the microwave cavity mode at 12.16 GHz via the magnon-photon coupling, which leads to the polariton gap.

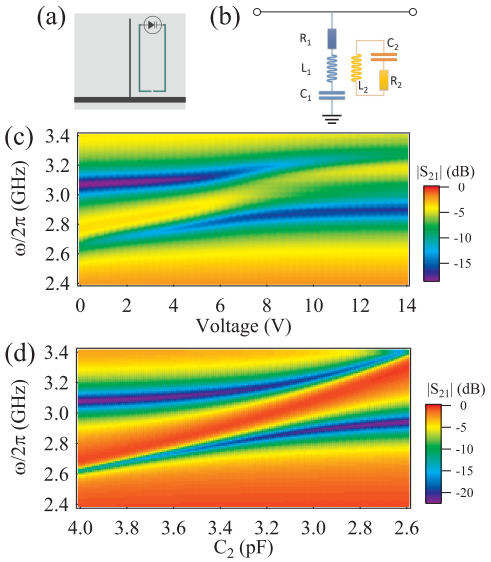

Fig. 2. (a)Schematic diagram of the metamaterial used to generate pseudo-magnon-polariton and (b) its effective LCR circuit. (c)Measured dispersion of a pseudo-magnon-polariton formed by using voltage-controlled metamaterials. At the external voltage of about 6.5 V, the pseudo-magnon-polariton gap induced by electrodynamic coupling in the metamaterial is observed, creating tunable electrodynamically induced transparency near 3 GHz. (d) Simulated dispersion by simply modelling the varactor as a variable capacitance.

the cavity mode is large, the FMR mode is only weakly excited by electromagnetic field. However, the amplitude of the FMR mode is significantly enhanced when it approaches the cavity mode. Consequently, the strong coupling of FMR mode and cavity modes generate hybridized photon-magnon quasi-particles, i.e., magnon polaritons. At $\mu_0 H_{ext} = 380$ mT corresponding to $\omega_1 = \omega_2$, the photon-like and magnon-like magnon polariton have equal amplitude and occur at $\omega_1 \pm \kappa$, respectively, with a magnon polariton gap of 2κ.

For comparison, we numerically calculated the $|S_{21}|$ coefficient using Eq. (3) with $\kappa/2\pi$ =78 MHz. The results are shown in Fig. 1(c), which has excellent agreement with the experimental results in Fig. 1(b), indicating the validation of our analytical model based on solution of the coupled LLG and Maxwell's equations.

B. Pseudo-Magnon Polariton

The development of metamaterials expands the classical photon-magnon coupling to new regimes, where the cavity mode is generated by an on-chip cut wire and the FMR mode in the ferromagnetic material is replaced by its metamaterial analogue, the split ring resonator (SRR). The SRR made by non-magnetic material can induce a microwave current when an external microwave magnetic field is applied, thus producing an effective magnetic response, which can be characterized by the resonant permeability of the metamaterial structure. [8] Using such an on-chip combination of metamaterials, a similar coupling effect is produced, generating the pseudo-magnon-polariton. Consequently, a voltage tunable EIT phenomenon is observed, allowing the propagation of microwave photon to be manipulated on-chip.

To demonstrate the pseudo-magnon-polariton, a metamaterial is designed as shown in Fig. 2(a). The cut wire is connected as shunt for the transmission line (with a characteristic impedance of Z_0=50 Ω), and its radiated microwave magnetic field induces microwave current in the SRR. When the two resonators have an equal resonance frequency, the mutual coupling hybridizes two resonances and generates the pseudo-magnon-polariton. The microwave response of such a metamaterial structure can be analyzed using transmission line models. As shown in Fig. 2(b), the series LCR circuit (L_1, C_1 and R_1) for the cut wire mutually couples with the RLC parallel circuit (L_2, C_2 and R_2) with resistance in series with the capacitor through the mutual inductance M. The resonance frequencies of the cut wire and the SRR are $\omega_1 = 1/\sqrt{L_1 C_1}$ and $\omega_2 = 1/\sqrt{L_2 C_2}$, respectively. One can tune the resonance frequency of the SRR by loading a varactor diode, whose capacitance can be varied by an external DC voltage.

The S_{21} parameter for this structure is obtained by solving for the net impedance of the circuit and using the transfer matrix. After simplification, the S_{21} parameter of the pseudo-magnon-polariton can be written as

$$S_{21} \approx 1 + \frac{Z_0/2L_1}{i(\omega - \omega_1) - \Delta\omega_1 + \frac{\kappa^2}{i(\omega-\omega_2)-\Delta\omega_2}}, \qquad (4)$$

where $\Delta\omega_1 \approx (2R_1 + Z_0)/4L_1$ and $\Delta\omega_2 \approx R_2/2L_2$ are the damping factors for the cut wire and the SRR respectively and $\kappa \approx M\omega/2\sqrt{L_1 L_2}$ is the coupling strength, which is linearly dependent on the mutual inductance M between the cut wire and the SRR. Equation (1) and (2) have the same expression

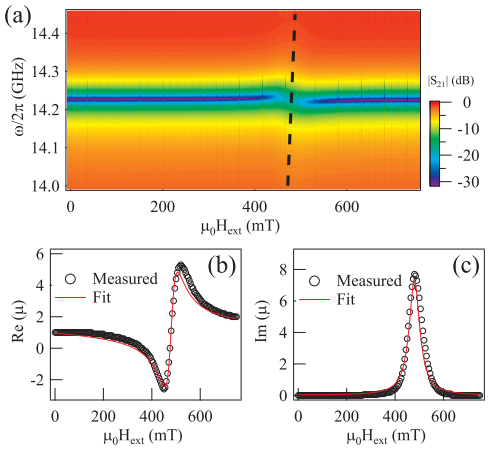

Fig. 3. (a) The transmission spectra of the MNP (28 mg) loaded cavity collected by successively changing the magnetic field. The dashed line refers to the FMR dispersion. Measured (symbols) real part (b) and imaginary part (c) of the permeability of the 5 nm diameter iron-oxide nanoparticles.

and indicate the similarity in origin for the magnon polariton and the pseudo-magnon-polariton.

Figure 2(c) shows the measured dispersion of a pseudo-magnon-polariton formed by using voltage-controlled metamaterials. When the frequency of the SRR is far from that of the cut wire, the amplitude of the resonance of the SRR is an order of magnitude weaker compared with that of the cut wire. At the external voltage of about 6.5 V the resonance frequency of the SRR is close to that of the cut wire, $\omega_1 \approx \omega_2 \approx 3.0$ GHz. Consequently, the gap (about 0.3 GHz) of the pseudo-magnon-polariton induced by electrodynamic coupling in the metamaterial is observed, creating EIT near 3 GHz. While the tunable EIT is also achievable for the magnon-polariton as shown in Figure 1, the pseudo-magnon-polariton in an on-chip metamaterial controlled by the DC voltage is more convenient for practical applications.

The dispersion of the pseudo-magnon-polariton has been calculated according to Eq. (4) as shown in Figure 2(d). Here $R_1 = 3.0\ \Omega$, $C_1 = 0.35$ pF and $L_1 = 8.0$ nH is deduced from the resonant S_{21} spectrum of the cut wire. Although the circuit of the varactor generally includes multiple electronic elements, we highlight the electrically tunable feature of the metamaterial structure by assuming that only the capacitance varies with the external applied DC voltage. The range of the capacitance C_2=4 pF to 2.6 pF is used for the calculation while $R_2 = 0.1\ \Omega$, $L_2 = 0.9$ nH and $M = 0.28$ nH are kept constant. The calculated result in Figure 2(d) is in agreement with the experimental observation. Notice that the capacitance of the varactor decreases with an increased voltage bias.

C. Characterization of the MNP

The coupling effect of magnon and photon is not only leading to a new field of cavity spintronics, but also providing a novel way to characterize the properties of magnetic materials and structures such as MNPs. Currently, MNPs are under extensive investigation for biomedical applications and an outstanding challenge here is how to accurately measure their complex permittivity and permeability for a milligram sample. This challenge has been addressed successfully based on the deep understanding of magnon-photon coupling [6]. Far from the FMR, the complex permittivity of the MNP is determined by the the shift of the cavity mode and the decrease of the quality(Q-) factor. In the vicinity of the FMR, an enhanced damping of the cavity photon is observed, which is different from the strong coupling effect for the low-damping YIG loaded cavity as shown in Figure 1. This so-called Purcell effect is due to the cavity photon coupled to the lossy magnon in the high damping MNPs, allowing the determination of the complex permeability. As shown in Figure 3(b) and (c) the deduced data (symbols) is in agreement with the theoretical calculation (solid lines).

III. Conclusion

In summary, we briefly review our recent work [9] in the field of cavity spintronics. An analytic expression has been developed to describe the magnon polariton dispersion based on the coupling between spin dynamics and cavity mode, which can well explain the hybridization of the cavity mode and FMR mode. We have also expanded the study to a new frontier: the pseudo-magnon-polariton, which is generated from the coupling between a voltage controlled split ring resonator, regarded as an artificial magnetic structure, and the cut wire resonator, an on-chip microwave resonator. Utilising the coupling of the photon and the magnon, the complex permeability for milligram MNP sample can be quantified.

Acknowledgement

This work has been funded by NSERC, CFI, the National Key Basic Research Program of China (2011CB925604), and the National Natural Science Foundation of China Grant No. 11429401.

References

[1] O. O. Soykal and M. E. Flatte, “Strong field interactions between a nanomagnet and a photonic Cavity”, Phys. Rev. Lett. 104, 077202, 2010.
[2] H. Huebl, C.W. Zollitsch, J. Lotze, F. Hocke, M. Greifenstein, A. Marx, R. Gross, and S.T.B. Goennenwein, “High Cooperativity in Coupled Microwave Resonator Ferrimagnetic Insulator Hybrids”, Phys. Rev. Lett. 111, 127003, 2013.
[3] Y. Tabuchi, S. Ishino, T. Ishikawa, R. Yamazaki, K. Usami, and Y. Nakamura, “Hybridizing Ferromagnetic Magnons and Microwave Photons in the Quantum Limit”, Phys. Rev. Lett. 113, 083603, 2014.
[4] X. Zhang, C.-L. Zou, L. Jiang, and H. X. Tang, “Strongly coupled magnons and cavity microwave photons”, Phys. Rev. Lett. 113, 156401, 2014.
[5] Lihui Bai, M. Harder, Y.P. Chen, X. Fan, J. Q. Xiao, and C.-M. Hu, “Spin pumping in electrodynamically coupled magnon-Pphoton systems”, Phys. Rev. Lett. 114, 227201, 2015.
[6] B. M. Yao, Y. S. Gui, M. Worden, T. Hegmann, M. Xing, X. S. Chen, W. Lu, Y. Wroczynskyj, J. van Lierop, C.-M. Hu, “Quantifying the complex permittivity and permeability of magnetic nanoparticles”, Appl. Phys. Lett. 106, 142406, 2015.
[7] D.R. Smith, J. B. Pendry, and M. C. K. Wiltshire “Metamaterials and Negative Refractive Index”, Science, 305, 788, 2004.
[8] J. B. Pendry, A. J. Holden, D. J. Robbins, W. J. Stewart, “Magnetism from conductors and enhanced nonlinear phenomena”, IEEE Trans. Microwave Theory Tech. 47, 2075 1999.
[9] For more information and references, please check our group website at: http://www.physics.umanitoba.ca/~hu/